UCSF
UC San Francisco Previously Published Works

Title

Resting-state functional connectivity and motor imagery brain activation

Permalink

https://escholarship.org/uc/item/946238td

Journal

Human Brain Mapping, 37(11)

ISSN

1065-9471

Authors

Saiote, Catarina
Tacchino, Andrea
Brichetto, Giampaolo
et al.

Publication Date

2016-11-01

DOI

10.1002/hbm.23280

Peer reviewed

Resting-State Functional Connectivity and Motor Imagery Brain Activation

Catarina Saiote,[1] Andrea Tacchino,[2] Giampaolo Brichetto,[2]
Luca Roccatagliata,[3] Giulia Bommarito,[4] Christian Cordano,[4]
Mario Battaglia,[2,5] Giovanni Luigi Mancardi,[4] and Matilde Inglese[1,4,6,7]*

[1]Department of Neurology, Icahn School of Medicine at Mount Sinai, New York
[2]Scientific Research Area, Italian MS Foundation (FISM), Genoa, Italy
[3]Department of Health Sciences (DISSAL), and Neuroradiology Department, IRCCS San
Martino University Hospital and IST, Genoa, Italy
[4]Department of Neuroscience, Rehabilitation, Ophthalmology, Genetics and Maternal and
Child Health (DINOGMI), University of Genoa, Genoa, Italy
[5]Department of Physiopathology, Experimental Medicine and Public Health, University of
Siena, Siena, Italy
[6]Department of Radiology, Icahn School of Medicine at Mount Sinai, New York
[7]Department of Neuroscience, Icahn School of Medicine at Mount Sinai, New York

◆ ━━━━━━━━━━━━━━━━━━━━━━━━━━━━━━━━ ◆

Abstract: Motor imagery (MI) relies on the mental simulation of an action without any overt motor execution (ME), and can facilitate motor learning and enhance the effect of rehabilitation in patients with neurological conditions. While functional magnetic resonance imaging (fMRI) during MI and ME reveals shared cortical representations, the role and functional relevance of the resting-state functional connectivity (RSFC) of brain regions involved in MI is yet unknown. Here, we performed resting-state fMRI followed by fMRI during ME and MI with the dominant hand. We used a behavioral chronometry test to measure ME and MI movement duration and compute an index of performance (IP). Then, we analyzed the voxel-matched correlation between the individual MI parameter estimates and seed-based RSFC maps in the MI network to measure the correspondence between RSFC and MI fMRI activation. We found that inter-individual differences in intrinsic connectivity in the MI network predicted several clusters of activation. Taken together, present findings provide first evidence that RSFC within the MI network is predictive of the activation of MI brain regions, including those associated with behavioral performance, thus suggesting a role for RSFC in obtaining a deeper understanding of neural substrates of MI and of MI ability. *Hum Brain Mapp* 37:3847–3857, 2016. © 2016 Wiley Periodicals, Inc.

Key words: motor imagery; fMRI; isochrony; functional connectivity; resting-state

◆ ━━━━━━━━━━━━━━━━━━━━━━━━━━━━━━━━ ◆

INTRODUCTION

Motor imagery (MI) is a mental process during which a movement is mentally simulated without any overt motor output [Jeannerod, 1995]. Task-based functional magnetic resonance imaging (fMRI) has led to substantial advances in our understanding of the neural substrates of MI, showing that the neural networks involved in MI overlap, to a considerable extent, with those recruited for the actual motor execution (ME), and include the dorsal premotor cortex (PmD), the supplementary motor area (SMA), and the intraparietal sulcus (IPS) and the supramarginal gyrus in the inferior parietal lobe (IPL). Furthermore, while some brain areas such as the prefrontal cortex, the posterior portion of the superior parietal lobe (SPL), the ventral premotor cortex (PmV) and the anterior SMA (pre-SMA) are more active during MI than ME, other brain regions such as the contralateral primary motor cortex (M1), the primary sensory cortex (S1), the SMA proper and the anterior SPL are more active during ME than MI [Gerardin et al., 2000; Grèzes and Decety, 2001; Guillot et al., 2012b; Hétu et al., 2013; Lotze and Halsband, 2006; Sharma and Baron, 2013; Stephan et al., 1995; Szameitat et al., 2012a,b].

Behavioral studies have shown that, in healthy adults, the actual execution and the mental rehearsal of the same movement share autonomic responses and temporal characteristics in terms of movement duration (i.e., mental isochrony), and that the spatio-temporal characteristics associated with ME and MI are affected by aging and disease status [Decety et al., 1989; Heremans et al., 2012; Saimpont et al., 2013; Tacchino et al., 2013]. Thus, chronometry tests designed to evaluate the temporal coupling between overt and simulated movements are regarded as a reliable method to assess the subjects' MI ability and performance [Guillot and Collet, 2005; Malouin et al., 2007].

Abbreviations

BOLD	Blood-oxygen-level dependent
CSF	Cerebrospinal fluid
DMN	Default mode network
fMRI	Functional magnetic resonance imaging
GLM	General linear model
HRF	Hemodynamic response function
IP	Index of performance
IPS	Intraparietal sulcus
KVIQ	Kinesthetic and Visual Imagery Questionnaire
LOC	Lateral occipital cortex
ME	Motor execution
MFG	Middle frontal gyrus
PFC	Prefrontal cortex
PmV	Ventral premotor cortex
RSFC	Resting-state functional connectivity
SFG	Superior frontal gyrus
SMA	Supplementary motor area
SPL	Superior parietal lobe
WM	White matter

Although task-induced functional imaging studies have contributed to the investigation of the neural correlates of the MI performance and practice [Guillot et al., 2008; Sharma et al., 2009], the extent to which intrinsic functional networks are related to MI task performance is poorly understood. Due to ease of implementation, resting-state studies are extremely attractive to be included in monitoring of progression or recovery from disease in clinical populations, often presenting with diversified types and severity of impairment. Therefore, it is of high interest to detect to which extent resting-state activity can predict a particular task and its behavioral correlates. Resting-state functional connectivity (RSFC) studies have shown that there is a considerable correspondence between functional networks during task-performance and intrinsic, coherent, low-frequency (<0.1 Hz) fluctuations in brain activity observed during rest [Cole et al., 2014; Smith et al., 2009]. In addition, Mennes and colleagues (2010) have reported that inter-individual differences in task-induced blood-oxygen-level dependent (BOLD) activity are predicted by the region's positive connectivity strength with the task-positive network or its negative connectivity with the default mode network (DMN). Furthermore, it has been suggested that neural activity during task performance and intrinsic neural activity are governed by a common mechanism [Cohen et al., 2008; Steyn-Ross et al., 2009]. However, the link between resting-state neural activity and task-related activity during MI is yet unknown, as well as its behavioral relevance.

Here, we investigated the relationship between RSFC and brain activity during ME and MI of a squeezing ball task with the following aims: (i) to investigate MI brain activity correlates of mental isochrony, (ii) to determine the relationship between RSFC and MI-related brain activity. Based on previous MI studies, we hypothesized that subjects with better mental isochrony would show differentiated recruitment of parietal and premotor regions [Guillot et al., 2008] and that higher RSFC with key MI regions would predict stronger recruitment of MI network during task performance [Hétu et al., 2013; Mennes et al., 2010].

METHODS

Subjects

Thirty-one healthy volunteers participated in the study (16 males; mean age $= 31.74 \pm 7.80$, range 21–53 years). All subjects were right-handed as assessed by Edinburgh Handedness Inventory [Oldfield, 1971] and none of them had previous history of neurologic or psychiatric illness. The study protocol was approved by the local Institutional Review Board and written informed consent was obtained from all subjects prior to participation.

Experimental Design and Motor Task

The experiment was performed in a single session including behavioral and MRI assessment. The tasks were

first performed outside of the scanner for behavioral scoring. First, all participants were instructed to perform the ME task, which required repeatedly squeezing a foam ball (7 cm diameter) at their own pace (in most cases at a rate of about 1 Hz) during a run of four blocks of 30s of ME separated by 30s of rest [Mizuguchi et al., 2013]. Next, they were instructed to "imagine" the same movement with a first person perspective during the MI run, using the same paradigm. After each block, the participants reported the number of movements they performed (overt during ME and imagined during MI). The tasks were then repeated during task-fMRI acquisition using the same paradigm but without behavioral assessment, that is, the participants did not report the number of movements during scanning. The subjects were informed of the start of each block via brief visual cues presented on a screen, visible through a mirror: a green circle marked the start of a task block and a red circle marked the start of a rest block (Supporting Information Fig. S1). The participants were asked to maintain the same pace throughout the experiment. The task-fMRI experiment was preceded by acquisition of resting-state fMRI (rs-fMRI). The order of MI and ME tasks was counterbalanced across subjects. Both tasks were performed first with the right hand and then with the left hand. For the sake of simplicity and given the exploratory nature of our study, only the data for the right hand are discussed.

Behavioral Data

Before MRI recording the following behavioral tests were administered to all subjects: (a) chronometry test [Decety et al., 1989; Tacchino et al., 2013], b) the Kinesthetic and Visual Imagery Questionnaire (KVIQ) [Malouin et al., 2007] and c) the Nine-hole peg test (9 HPT) [Grice et al., 2003]. The chronometry test was used to measure the isochrony between ME and MI. The number (reported by the subjects) of executed (#ME) and imagined (#MI) ball squeezes per block was recorded and the ratio between the average number of movements of the overt and mental tasks was computed for each hand (#ME/#MI). Since the ideal ratio is 1 (equal duration of MI and ME), both values below 1 (faster MI than ME) or above 1 (faster ME than MI) represent deviations from the ideal score. As such, we computed an index of performance (IP) as the absolute difference between the calculated ratio and the ideal score: $IP = |1 - \#ME/\#MI|$. We and used the IP as our behavioral measure of interest, as it is considered a reliable and objective measure of MI accuracy and an indicator of motor system integrity [Collet et al., 2011; Guillot et al., 2012a; Guillot and Collet, 2005; Di Rienzo et al., 2014]; and the outcome corresponds specifically to the task that was performed during fMRI (additional information in the Supplementary Material). The KVIQ was used to rate the vividness of imagery abilities. The KVIQ-20 is a questionnaire developed to measure the vividness of each dimension of motor imagery (visual and kinesthetic) on a five-point ordinal scale (5 = vivid imagery, 1 = no imagery) [Malouin et al., 2007]. The 9 HPT is a measure of motor dexterity. In this test, participants have to place nine pegs one at a time into nine holes of a wooden board a then remove them again. Participants performed the 9 HPT test twice with each hand and the time needed to complete the test was measured and averaged [Grice et al., 2003].

MATLAB (version R2011a, The MathWorks, Inc., Natick, MA, United States) was used to analyze the behavioral data. Spearman's correlation coefficient was used to measure the association between the IP and the KVIQ and correlations between age and the behavioral scores and results were considered statistically significant if $P < 0.05$.

MRI Acquisition

All subjects underwent MRI at 1.5T (SignaHDxt scanner, GE MEDICAL Systems), using an 8-channel transmit/receive head coil. The MRI protocol included the following sequences: a) axial PD-T2-weighted (TR/TE1/TE2 = 2340/102/38.25 ms; FA = 90°; voxel size = 0.94 × 0.94 × 4 mm³); b) sagittal 3DT1-weighted FSPGR (TR/TE/TI = 11.56/5.048/500 ms; FA = 8°, voxel size = 1 × 1 × 1 mm³); c) gradient-echo Echo Planar Imaging (EPI) sensitive to BOLD signal with 150 volumes for resting-state fMRI (TR/TE = 3000/60 ms; FA = 90°, slice spacing: = 1 mm, voxel size = 3.3 × 3.3 × 3.3 mm³; d) gradient-echo EPI with 83 volumes for each of the 4 task-fMRI runs (TR/TE = 3000/60 ms; FA = 90°, slice spacing = 1 mm, voxel size = 3.75 × 3.75 × 4 mm³). During rs-fMRI, participants were explicitly instructed to keep their eyes closed, to relax and to move as little as possible.

fMRI Pre-Processing

Initial pre-processing steps of slice-timing correction for regular ascending acquisition (with Fourier-space time series phase-shifting) and despiking (detection and reduction of extreme time series outliers by fitting a smooth curve insensitive to extreme outliers to the data) were performed in AFNI (http://afni.nimh.nih.gov). All other pre-processing steps were performed using FSL (FMRIB's Software Library, www.fmrib.ox.ac.uk/fsl) [Jenkinson et al., 2012; Smith et al., 2004] as implemented in FEAT [Woolrich et al., 2001, 2009], including: removal of the first 3 volumes, motion correction using MCFLIRT [Jenkinson et al., 2002], non-brain removal using BET [Smith, 2002], spatial smoothing (Gaussian kernel, FWHM = 6 mm), grand-mean intensity normalization of all volumes by a single multiplicative factor, and high-pass temporal filtering (Gaussian-weighted least-squares straight line fitting, sigma = 30s for task-fMRI and sigma = 50s for rest-fMRI). Nuisance signal from white matter (WM) and cerebrospinal fluid (CSF) was calculated by segmenting T1-weighted images with FAST, then registering the resulting WM and CSF masks

to functional space and averaging the raw time series within each mask. Additional information regarding the choices of preprocessing steps can be found in the Supplementary Material.

Task-fMRI Analysis

To detect task-related activity, one explanatory variable (EV) was defined to model the On-Off periods of the task for each run (ME or MI) and convolved with the hemodynamic response function (HRF). The six motion parameters calculated during motion correction were added as confound EVs. Mean CSF and WM signals were added to the general linear model (GLM) as covariates of no interest. Two contrasts were defined to obtain individual maps of activation and deactivation related to each of the two tasks: ME and MI with the right hand. Individual functional images were registered to corresponding T1-weighted images using Boundary-Based Registration [Greve and Fischl, 2009]. Then, linear affine (12 DOF) registration of each subject's high-resolution T1-weighted image to standard-space (MNI152 brain template, 2 mm^3 resolution) was performed with FLIRT [Jenkinson et al., 2002].

Individual activation maps were used for several group-level analyses performed using mixed-effects model as implemented in FSL FLAME. One-sample t-tests were used to model the group mean for each task, with age as a covariate. Two-sample paired t-tests were used to obtain group comparisons of ME and MI. Results were converted to Z-values and then thresholded at $Z = 2.3$ for cluster formation and significance threshold corrected for multiple voxel comparisons ($P < 0.05$) and further corrected for six MI and ME comparisons using Bonferroni correction.

Additionally, correlations between MI activation and the IP, and between the 9 HPT scores and ME were modeled separately, with age as a covariate. Z-maps were thresholded at $Z = 2.3$ for cluster formation and significance threshold corrected for multiple voxel comparisons ($P < 0.05$) and further corrected for four MI and four ME correlation tests using Bonferroni correction.

Rs-fMRI Analysis

Seeds were created as spheres of 6 mm radius centered in regions of interest (ROIs) reported in the literature to be relevant for motor imagery (Supporting Information Fig. S2) [Gerardin et al., 2000; Guillot et al., 2008; Jeannerod, 1995; Lotze, 2013] with coordinates functionally defined according to group mean MI activation: the SMA (-6, -4, 66), pre-SMA (4, 24, 48), left ($-58, -38, 30$) and right IPL (58, $-38, 30$), left ($-44, -6, 54$) and right PmD (44, $-6, 54$), left PmV ($-54, 6, 20$), and left SPL ($-38, -50, 54$); and group ME activation: left M1 ($-36, -28, 54$). Each ROI was created in the standard space 2 mm MNI template and then registered to the individual native functional space and used to

average a mean timeseries from the pre-processed data. Then, to obtain individual RSFC maps for each ROI, the preprocessed rs-fMRI data were entered into a first-level GLM analysis as implemented in FEAT, with the mean ROI timeseries used as an EV and the 6 motion parameters, WM and CSF mean signals as covariates of no interest. Next, to create a resting-state MI network, the RSFC maps of all ROIs (except the M1) were averaged for each subject.

Correspondence Between RSFC and MI-Related BOLD Activity

To investigate the relationship between inter-individual differences in RSFC within the MI network and inter-individual differences in MI BOLD activity, a voxel-matched linear regression analysis was performed using FSL FLAME, between the individual task parameter estimates of MI task-fMRI and the individual RSFC maps of the MI network, entered as a voxelwise covariate. The task parameter estimates were entered as dependent variables and RSFC maps as voxelwise EVs, after being transformed to standard space and concatenated to a 4D file, adapting the approach described by Mennes et al., (2010). To evaluate generalizability of the approach, the same analysis was performed to correlate ME-related BOLD activity with the RSFC within the ME network as described in the Supplementary Material. The results were converted to Z-values as described above and then cluster corrected for multiple comparisons with Gaussian random field theory ($Z > 2.0$; $P < 0.05$) and further corrected for four MI and four ME correlations with RSFC using Bonferroni correction.

RESULTS

Behavioral Results

All participants completed the ME and MI task. KVIQ scores were in the range expected for healthy subjects (mean $= 137.97 \pm 20.17$), with slightly better values for the visual KVIQ (mean $= 72.77 \pm 9.53$) than the kinesthetic KVIQ (mean $= 65.19 \pm 14.42$) [Malouin et al., 2007]. MI movements (mean #MI $= 21.25 \pm 12.51$) were significantly slower (paired t-test: t(30)=5.8563, $P = 2.0851e-06$) that ME (mean #ME $= 25.96 \pm 9.86$) movements (mean #ME/#MI $=1.23 \pm 0.25$) with only two subjects showing results lower than 1 and a resulting IP score between 0.036 and 1.038. (mean $= 0.250 \pm 0.231$). Values for the 9 HPT were within expected range for this sample (mean $= 18.67 \pm 2.27$ s) [Grice et al., 2003]. No statistically significant correlations were found between age and the IP scores, ($\rho = -0.25$, $P = 0.17$) or between age and the 9 HPT ($\rho = 0.20$, $P = 0.29$). There was no statistically significant association between KVIQ scores and age [KVIQ-V ($\rho = -0.33$, $P = 0.07$); KVIQ-K ($\rho = -0.24$, $P = 0.20$) and total KVIQ ($\rho = -0.30$, $P = 0.11$)] and between the IP and KVIQ scores
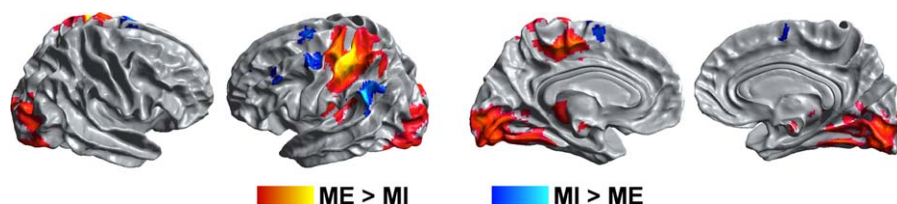
ME > MI   **MI > ME**

Figure 1.

Comparison of brain activation during MI and ME. ME-predominant activity was found in the contralateral M1, putamen and thalamus, SMA, premotor cortex and the visual cortex (ME > MI, shown in red-yellow); MI-predominant activity was found in the pre-SMA, bilateral lateral frontal regions, anterior insula and parietal regions (MI > ME, shown in blue). Results are cluster corrected for multiple comparisons ($Z > 2.3$; $P < 0.0083$) and are shown overlaid on the MNI template.

[KVIQ-V ($\rho = 0.22$, $P = 0.23$); KVIQ-K ($\rho = 0.05$, $P = 0.80$) and total KVIQ ($\rho = 0.10$, $P = 0.59$)].

ME and MI Task-fMRI

Both ME and MI activated similar motor networks (Supporting Information Fig. S3), which included contralateral primary motor areas, lateral and medial premotor areas. In both tasks, significantly reduced task activation compared to baseline blocks was found in the medial PFC (anterior cingulate and paracingulate gyri). Also, in case of MI, bilateral V1 and V2 and, in case of ME, the contralateral M1 showed significantly reduced activation.

The contrast ME > MI showed that, in comparison with MI, there is significantly higher activation during ME in the contralateral M1 and primary sensory cortex (S1), medial premotor (precentral gyrus and SMA), left superior parietal areas, left secondary somatosensory areas (parietal and central opercular cortex) and bilateral visual cortex; in the contralateral thalamus, putamen and pallidum; and bilateral lobules I – V of the cerebellum and contralateral lobules VI – IX. The opposite contrast, MI > ME, showed that activation is higher during imagery in the following regions: left superior frontal gyrus (SFG) and middle frontal gyrus (MFG) and dorsomedial premotor areas (paracingulate gyrus or pre-SMA), and left lateral occipital cortex (LOC) and IPL (angular and supramarginal gyrus) (Fig. 1, Table I).

Correlation of Task-fMRI With Behavioral Scores

Index of performance (IP)

The IP correlated positively with brain activity in the left SPL (7A-7PC, left anterior IPS, left precuneus, and in the right dorsolateral and ventrolateral prefrontal cortex (PFC) (MFG and inferior frontal gyrus) (Fig. 2A, red-yellow). Negative correlations between the IP and MI activity were found in the left secondary somatosensory cortex (central opercular and insular cortex) and primary auditory cortex (Heschl's gyrus) (Fig. 2A, blue). There were no significant correlations between the IP scores and brain activity during ME.

Nine-hole peg test (9 HPT)

Brain activity during ME correlated positively with 9 HPT scores in the right middle and superior frontal gyri, right dorsal premotor regions, anterior and posterior cingulate gyrus and precuneus, bilateral central opercular and insular cortex, right putamen and thalamus bilaterally, meaning that higher activation of these areas during motor task was associated with less optimal performance in the 9 HPT score (Fig. 2B).

RSFC-Task Correlations With Seed-Based Approach

Higher RSFC within the MI network correlated with higher activation in several regions on the left hemisphere, such as the SMA, SM1, central opercular cortex, and superior temporal gyrus, as well as in the medial M1, and right PmD (Fig. 3). In addition, inter-individual differences in RSFC predicted task-evoked activation in the left SPL, angular gyrus (IPL) and IPS.

In order to test the specificity of our method for the MI network, we repeated the analysis using as control seed for RSFC the left M1, which is robustly activated in ME but rarely in MI. As expected, we did not find any significant correlation between left M1 RSFC and brain activity during MI. Conversely, higher RSFC with the left M1 was associated with higher activity of the left SM1, bilateral SMA and lateral premotor regions during ME.

Correlation between ME-related activation and RSFC within the ME network was significant in regions overlapping ME activation in the left SM1, bilateral PmD, left SMA, medial M1, and left parietal and central opercular cortex (Supporting Information Fig. S4).

DISCUSSION

To our knowledge, this is the first study that sought to characterize the association between inter-individual

TABLE I. Peak of activations of the comparisons between MI and ME. Activated regions were labeled using the SPM Anatomy toolbox (Eickhoff et al., 2007, 2005)

Location	Cytoarchitectonic location	MNI coordinates			Z-score
		x	y	z	
MI > ME					
L Angular Gyrus		−44	−50	30	3.35
L Middle Frontal Gyrus		−32	64	10	3.78
L Precentral Gyrus		−42	2	56	3.95
L SMA		−10	4	64	3.51
L Superior Frontal Gyrus		−16	8	68	4.05
L Superior Parietal Lobule	7A	−32	−70	52	4.12
L SupraMarginal Gyrus	IPL (PFm)	−62	−54	26	4.48
ME > MI					
L Calcarine Gyrus	hOC1 [V1]	−8	−92	8	5.81
L Caudate Nucleus		−20	−24	20	3.37
L Paracentral Lobule	4a	−8	−24	50	5.89
L Postcentral Gyrus	4a	−42	−26	60	8.20
L Postcentral Gyrus	4p	−36	−28	54	8.37
L Postcentral Gyrus	2	−48	−30	54	7.98
L Precentral Gyrus		−28	−20	64	5.89
L Putamen		−28	−12	2	4.35
L Rolandic Operculum		−46	−22	22	5.55
L SMA		−4	−12	52	5.61
L Thalamus	Motor	−16	−22	2	5.74
L Thalamus	Prefrontal	−16	−22	8	5.4
R Cerebellum (lobule V)		4	−52	−2	6.89
R Cerebellum (lobule VI)		16	−54	−16	8.29
R Cerebellum (lobule VIII)		18	−62	−46	6.83

differences in task-evoked brain activity during MI and inter-individual differences in baseline intrinsic functional connectivity during rest. Our findings are in agreement with previous work that investigated the temporal characteristics of MI and extend these results by showing the relationship between an index of execution and imagery isochrony, the underlying brain correlates during MI and the corresponding intrinsic functional connectivity in the MI network.

In support of our hypothesis, we found a significant correlation between MI ability measured as mental chronometry (IP score) and the activation of the left parietal lobe and right prefrontal regions. Previous studies and ours support the crucial role of the left parietal lobe for the generation of mental images and planning required for MI [Guillot et al., 2008; Sirigu et al., 1996] and the importance of the fronto-parietal network for internal movement representation and cognitive control [Gerardin et al., 2000; Hétu et al., 2013]. This is not surprising considering the established importance of the parietal cortex for visuomotor integration, spatial information, attention and goal selection during complex tasks [Culham and Valyear, 2006; Jackson and Husain, 2006; Rushworth et al., 2003], and in light of its anatomical connection with the premotor and motor cortex [Fogassi and Luppino, 2005]. Sirigu et al., (1996) showed that in patients with lesions restricted to the parietal lobe, the ability to predict the duration of a

movement through imagery was impaired in comparison to healthy controls and to patients with lesions in primary motor areas. Skoura et al., (2009) demonstrated that in children, the improvement of isochrony with age might be related to maturation of the parietal and prefrontal cortices [Skoura et al., 2009]. Our results show that higher IP scores (deviation from the ideal ratio of 1 that reflects equal duration of MI and ME) correspond to an increase in parietal activation. Higher IP scores might reflect greater effort in performing the imagery task with a consequent need for a greater neural recruitment, considering that this correlation was found during MI performance in the scanner and not during ME. Although the behavioral scores were not obtained simultaneously with fMRI acquisition, these results are somehow unexpected, considering that in a previous study, Guillot et al., (2008) reported higher activation of bilateral parietal regions in good imagers when compared to poor imagers. However, they used a composite score including not only chronometry measures, but also questionnaires of MI ease and vividness, and autonomic responses (skin conductance), preventing a more direct comparison with our results. In addition, our subjects did not differ in terms of performance on the KVIQ scale and, therefore, we could not identify a subgroup of poor imagers. Although mental chronometry is regarded as a reliable test to probe individuals' imagery ability in a more sensitive and quantifiable
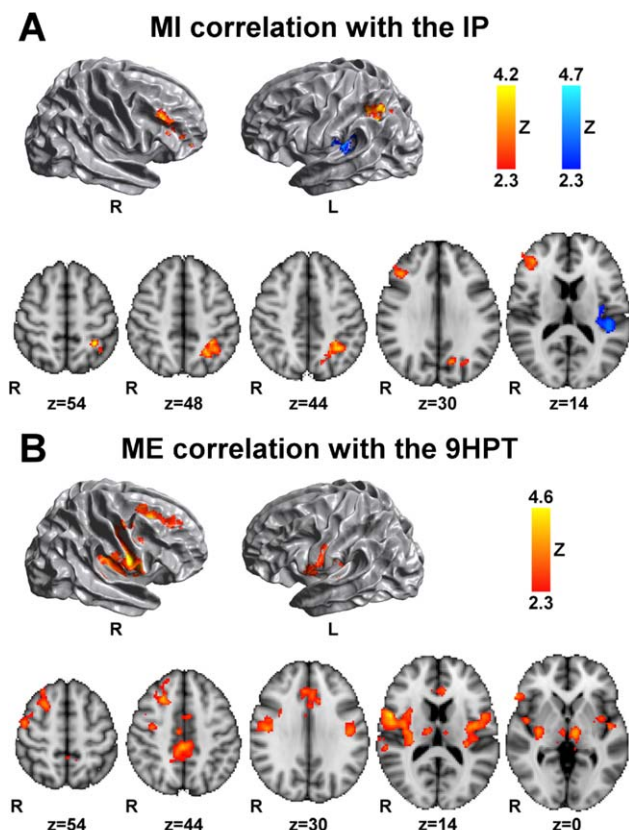
Figure 2.

Correlation between brain activity and behavioral measures. (**A**) During MI the IP correlates positively (red-yellow) with brain activity in regions of the right PFC, left SPL and IPS, and left precuneus, and correlates negatively (blue) with the left central opercular and insular cortex, and Heschl's gyrus. (**B**) During ME, the 9 HPT correlates with ME brain activity in PFC, premotor regions, anterior and posterior cingulate gyrus, precuneus, bilateral central opercular, insular cortex and thalamus, and right putamen. Results are cluster corrected for multiple comparisons ($Z > 2.3$; $P < 0.0125$), and are shown overlaid on the MNI template.

manner, it lacks information about MI vividness and difficulty. Moreover, it is task-dependent, and perhaps more suited for monitoring the temporal characteristics of motor actions during the performance of complex movements rather than during blocks of single simple movements.

Our results show that MI movements were on average significantly slower than ME. The most common cause for overestimation of movement duration in healthy adults is task complexity, which cannot account for increased MI duration in our case. Instead, simple movements are expected to have very similar duration in MI and ME, and only long movements (over 30s duration) are expected to be underestimated during MI ([Guillot et al., 2012a; Guillot and Collet, 2005]. However, overestimation of the duration of simple movements by healthy adults has been reported

before by Lebon and colleagues (2012) with a previously practiced thumb to finger opposition sequence task in both good and poor imagers; Stinear and colleagues (2007) in a task requiring a sequence of arm movements resembling a cross, and a thumb to finger opposition task both with the left and right hands; and Sabaté and colleagues (2004) in finger tapping sequences of increasing difficulty, in both hands, in both younger adults (mean age ± S.E: 30.7 ± 2.9 years) and older adults (mean age ± S.E: 52.9 ± 4.3 years). What is common between the mentioned examples is that these simple movements were repeated several times creating a block of relatively long duration (20s in Lebon et al., (2012), 30s in our case and in Stinear et al. (2007), and 10 repetitions of the sequence in Sabaté et al., (2004)). Thus, it seems that this particular design might also lead to overestimation of movement duration during MI. Another possible explanation for longer MI duration in our results is the need for the participants to count how many movements they are performing during MI, which might increase the mental effort, by forcing two different mental tasks to take place simultaneously: MI itself and internal counting.

As expected, we did not find a significant correlation between mental chronometry and the KVIQ scores [Lebon et al., 2012] and we found a trend for worsening visual KVIQ scores with increasing age compared to kinesthetic KVIQ, previously noted in the literature [Saimpont et al., 2013].

Higher activation during ME in several motor regions was associated with worse performance in the 9 HPT, which could possibly be interpreted as increased motor or attentional effort. Although the 9 HTP requires a level of dexterity not matched by the press-ball task performed in the scanner, it can more generally be regarded as a measure of upper extremity motor function [Grice et al., 2003; Wang et al., 2011], sensitive to minor impairment in several neurologic conditions. Therefore, it will be interesting to know how comparable the results are in clinical populations where the 9 HPT is a standard evaluation tool [Beebe and Lang, 2009; Cohen et al., 2000; Earhart et al., 2011].

The most novel aspect of our study is the finding that RSFC within the MI network predicted MI task-activation in the parietal cortex and premotor areas. Previous studies comparing resting-state and task networks have highlighted that, in spite of a correspondence, RSFC cannot fully characterize and account for task-evoked activation [Cole et al., 2014; Mennes et al., 2010, 2013; Smith et al., 2009], and particularly that networks recruited during tasks involving higher order cognitive functions are more closely related to RSFC than those involving subcortical networks, the limbic or primary cortices [Mennes et al., 2013]. Therefore, the higher level of cognitive effort required during imagery compared to simple motor tasks might explain our results of greater correspondence with parietal areas involved in cognitive processes and premotor regions relevant for planning, rather primary motor functions. The clusters of significant correlation were
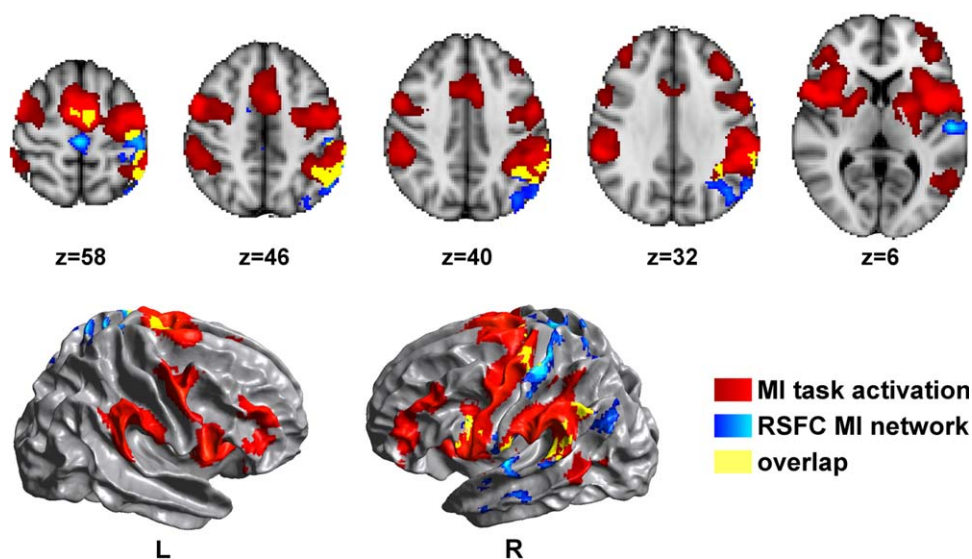
Figure 3.

Regions where inter-individual differences in RSFC within the MI network predict activation during MI. Higher RSFC within the MI network (blue) correlated with higher activation in several regions, such as the left SMA, SM1, SPL, angular gyrus, IPS, central opercular cortex and superior temporal gyrus, as well as in the medial M1, overlapping (yellow) or adjacent with mean MI activation (red). Results are cluster corrected for multiple comparisons ($Z > 2.0$; $P < 0.0125$), and are shown overlaid on the MNI template.

either overlapping or adjacent to regions of MI task-evoked activation suggesting that inter-individual differences in intrinsic connectivity of the MI network partly account for the individual variability in recruiting additional brain regions to perform the same MI task. Although MI training has been shown to impact RSFC [Ge et al., 2014; Zhang et al., 2014], the relationship between baseline RSFC and MI activation had not been studied before. Interestingly, the recruitment of regions that were correlated with the IP score in the left parietal lobe was predicted by RSFC within the MI network. Although the difference in visual input (eyes-open during task-fMRI and eyes closed during rs-fMRI) could have confounded the RSFC-task correspondence, primary visual areas were not part of the regions used to create the MI network. In addition, we did not find any correlations between MI-activation and rs-fMRI in the visual cortex, suggesting that the confounding effect, if any, was negligible.

There has been considerable debate regarding the involvement of the M1 in motor imagery, and previous studies suggested that the M1 is not consistently recruited across individuals, possibly due to variations in ME or MI skill, or even MI modality [Dechent et al., 2004; Guillot et al., 2008; Hétu et al., 2013]. Using our approach, we tested the differential involvement of the M1 in MI and ME, and did not find a significant correlation between MI-evoked brain activity and RSFC with the M1. However, task-evoked activation of motor regions during ME was predicted by inter-individual differences in RSFC with the M1. These results confirm both the specificity of our findings with the MI network RSFC and the limited involvement of the M1 during MI in healthy subjects. Results of ME task activation with ME network RSFC (Supporting Information) support generalizability of the approach used here.

One limitation of our study is the lack of monitoring of overt movement during MI (for instance, using electromyography), particularly during fMRI acquisition. Also, we did not acquire physiologic measures of MI performance (skin conductance) or subjective ratings specific to our task, which would have provided a more comprehensive assessment of participants MI abilities. In addition, although chronometry provides an objective quantitative measure of MI ability and the IP was in our case the measure best related to the task performed during fMRI, it does not probe aspects such as vividness and ease of performance. Thus, future studies should be conducted with composite measures for a comprehensive assessment of MI in all its complexity, ideally during scanning. Lastly, not only may the movement counting have delayed MI as mentioned above, but it is also not entirely possible to disentangle the MI activation correlated with the IP and with the counting effort. Indeed, the parietal cortex is known to be involved in mathematical operations [Fehr et al., 2007; Piazza and Izard, 2009] and an improved design in future studies should assess chronometry without counting.

MI practice has been used to improve motor performance among athletes and musicians [Di Rienzo et al., 2014] and to enhance recovery of motor functions in patients

affected by several neurological diseases such as stroke [Butler and Page, 2006; Sharma et al., 2009; Szameitat et al., 2012a], Parkinson's disease [Helmich et al., 2012], complete spinal cord injury [Cramer et al., 2007] and limb amputation [Raffin et al., 2012]), often combined with neurofeedback approaches [Blefari et al., 2015; Boe et al., 2014]. Interestingly, the representation of movements remains possible after central nervous system (CNS) injury. For instance, it has been shown that patients with stroke, even with severe disease, can perform a rehearsal of imagined motor actions with the same accuracy and vividness of healthy subjects [Johnson et al., 2002]. This suggests that mental movement representation is not dependent on motor activity following CNS injury and that MI is a pre-morbid trait unrelated to cerebral damage [Guillot et al., 2008]. In addition, several studies have shown that the degree of motor recovery is partly determined by the individuals' ability to generate mental images [Guillot et al., 2004; Mizuguchi et al., 2015; Simmons et al., 2008]. There is, however, considerable inter-subject variability in MI ability which has been associated with different patterns of MI fMRI brain activation [Charlot, 1992; Guillot et al., 2008]. Since individual differences in MI ability can influence fMRI brain activation during MI and recovery following a CNS injury, it is crucial to identify and stratify individuals who can benefit from MI practice [Blefari et al., 2015; Sharma et al., 2006; Simmons et al., 2008]. The most common tools currently used to test patient's MI abilities are self-rating questionnaires that assess the subjective imagery vividness [Malouin et al., 2007], and are thus limited by the intrinsic variability associated with subjective ratings. There is, therefore, the need of additional objective measures of MI ability and of a deeper understanding of neural substrates of the diverse aspects of MI ability. Our results show that inter-individual differences in RSFC of the MI can partly account for differences in activation of several MI regions, some of them with known relevance in MI ability. Considering the exploratory nature of this study and the number of multiple comparisons, our findings need to be validated in larger samples, as well as with more complex motor imagery tasks and with comprehensive behavioral assessment. Exploring the relationship between alterations in RSFC of clinical groups and changes in MI ability and brain activity might be a relevant future avenue of research. It would be interesting to determine whether RSFC-based studies could contribute to identify patients, who could best benefit from neurorehabilitation treatments, or whether RSFC with selected brain areas with meaningful behavioral impact might be explored as a possible treatment target to improve MI ability by means of neurofeedback or brain stimulation approaches in combination with MI practice.

REFERENCES

Beebe JA, Lang CE (2009): Relationships and responsiveness of six upper extremity function tests during the first six months of recovery after stroke. J Neurol Phys Ther 33:96–103.

Blefari ML, Sulzer J, Hepp-Reymond M-C, Kollias S, Gassert R (2015): Improvement in precision grip force control with self-modulation of primary motor cortex during motor imagery. Front Behav Neurosci 9:1–11.

Boe S, Gionfriddo A, Kraeutner S, Tremblay A, Little G, Bardouille T (2014): Laterality of brain activity during motor imagery is modulated by the provision of source level neuro-feedback. Neuroimage 101:159–167.

Butler AJ, Page SJ (2006): Mental Practice With Motor Imagery: Evidence for Motor Recovery and Cortical Reorganization After Stroke. Arch Phys Med Rehabil 87:2–11.

Charlot V (1992): Different mental imagery abilities result in different regional cerebral blood flow activation patterns during cognitive tasks. Neuropsychologia 30:565–580.

Cohen AL, Fair D. a, Dosenbach NUF, Miezin FM, Dierker D, Van Essen DC, Schlaggar BL, Petersen SE (2008): Defining functional areas in individual human brains using resting functional connectivity MRI. Neuroimage 41:45–57.

Cohen JA, Fischer JS, Bolibrush DM, Jak AJ, Kniker JE, Mertz LA, Skaramagas TT, Cutter GR (2000): Intrarater and interrater reliability of the MS functional composite outcome measure. Neurology 54:802–806.

Cole MW, Bassett DS, Power JD, Braver TS, Petersen SE (2014): Intrinsic and task-evoked network architectures of the human brain. Neuron 83:238–251.

Collet C, Guillot A, Lebon F, MacIntyre T, Moran A (2011): Measuring motor imagery using psychometric, behavioral, and psychophysiological tools. Exerc Sport Sci Rev 39:85–92.

Cramer SC, Orr ELR, Cohen MJ, Lacourse MG (2007): Effects of motor imagery training after chronic, complete spinal cord injury. Exp Brain Res 177:233–242.

Culham JC, Valyear KF (2006): Human parietal cortex in action. Curr Opin Neurobiol 16:205–212.

Decety J, Jeannerod M, Prablanc C (1989): The timing of mentally represented actions. Behav Brain Res 34:35–42.

Dechent P, Merboldt K-D, Frahm J (2004): Is the human primary motor cortex involved in motor imagery? Brain Res Cogn Brain Res 19:138–144.

Earhart GM, Cavanaugh JT, Ellis T, Ford MP, Foreman KB, Dibble L (2011): The 9-Hole Peg Test of Upper Extremity Function. J Neurol Phys Ther 35:157–163.

Eickhoff SB, Stephan KE, Mohlberg H, Grefkes C, Fink GR, Amunts K, Zilles K (2005): A new SPM toolbox for combining probabilistic cytoarchitectonic maps and functional imaging data. Neuroimage 25:1325–1335.

Eickhoff SB, Paus T, Caspers S, Grosbras MH, Evans AC, Zilles K, Amunts K (2007): Assignment of functional activations to probabilistic cytoarchitectonic areas revisited. Neuroimage 36:511–521.

Fehr T, Code C, Herrmann M (2007): Common brain regions underlying different arithmetic operations as revealed by conjunct fMRI-BOLD activation. Brain Res 1172:93–102.

Fogassi L, Luppino G (2005): Motor functions of the parietal lobe. Curr Opin Neurobiol 15:626–631.

Ge R, Zhang H, Yao L, Long Z (2014): Motor imagery learning induced changes in functional connectivity of the default mode network. IEEE Trans Neural Syst Rehabil Eng 23:138–148.

Gerardin E, Sirigu A, Lehéricy S, Poline JB, Gaymard B, Marsault C, Agid Y, Le Bihan D (2000): Partially overlapping neural networks for real and imagined hand movements. Cereb Cortex 10:1093–1104.

◆ Saiote et al. ◆

Greve DN, Fischl B (2009): Accurate and robust brain image alignment using boundary-based registration. Neuroimage 48:63–72.

Grèzes J, Decety J (2001): Functional anatomy of execution, mental simulation, observation, and verb generation of actions: A meta-analysis. Hum Brain Mapp 12:1–19.

Grice KO, Vogel K. a, Le V, Mitchell A, Muniz S, Vollmer MA (2003): Adult norms for a commercially available nine hole peg test for finger dexterity. Am J Occup Ther 57:570–573.

Guillot a, Collet C, Dittmar a (2004): Relationship between visual and kinesthetic imagery, field dependence-independence, and complex motors skills. J Psychophysiol 18:190–198.

Guillot A, Collet C (2005): Duration of mentally simulated movement: A review. J Mot Behav 37:10–20.

Guillot A, Collet C, Nguyen VA, Malouin F, Richards C, Doyon J (2008): Functional neuroanatomical networks associated with expertise in motor imagery. Neuroimage 41:1471–1483.

Guillot A, Hoyek N, Louis M, Collet C (2012a): Understanding the timing of motor imagery: Recent findings and future directions. Int Rev Sport Exerc Psychol 5:3–22.

Guillot A, Di Rienzo F, MacIntyre T, Moran A, Collet C (2012b): Imagining is Not Doing but Involves Specific Motor Commands: A Review of Experimental Data Related to Motor Inhibition. Front Hum Neurosci 6:1–22.

Helmich RC, Bloem BR, Toni I (2012): Motor imagery evokes increased somatosensory activity in Parkinson's disease patients with tremor. Hum Brain Mapp 33:1763–1779.

Heremans E, D'Hooge AM, De Bondt S, Helsen W, Feys P, D'hooge A-M, De Bondt S, Helsen W, Feys P (2012): The relation between cognitive and motor dysfunction and motor imagery ability in patients with multiple sclerosis. Mult Scler J 18:1303–1309.

Hétu S, Grégoire M, Saimpont A, Coll MP, Eugène F, Michon PE, Jackson PL (2013): The neural network of motor imagery: An ALE meta-analysis. Neurosci Biobehav Rev 37:930–949.

Jackson SR, Husain M (2006): Visuomotor functions of the posterior parietal cortex. Neuropsychologia 44:2589–2593.

Jeannerod M (1995): Mental imagery in the motor context. Neuropsychologia 33:1419–1432.

Jenkinson M, Bannister P, Brady M, Smith S (2002): Improved Optimization for the Robust and Accurate Linear Registration and Motion Correction of Brain Images. Neuroimage 17:825–841.

Jenkinson M, Beckmann CF, Behrens TEJ, Woolrich MW, Smith SM (2012): Fsl. Neuroimage 62:782–790.

Johnson SH, Sprehn G, Saykin AJ (2002): Intact Motor Imagery in Chronic Upper Limb Hemiplegics: Evidence for Activity-Independent Action Representations. J Cogn Neurosci 14:841–852.

Lebon F, Byblow WD, Collet C, Guillot A, Stinear CM (2012): The modulation of motor cortex excitability during motor imagery depends on imagery quality. Eur J Neurosci 35:323–331.

Lotze M (2013): Kinesthetic imagery of musical performance. Front Hum Neurosci 7:280.

Lotze M, Halsband U (2006): Motor imagery. J Physiol Paris 99:386–395.

Malouin F, Richards CL, Jackson PL, Lafleur MF, Durand A, Doyon J (2007): The Kinesthetic and Visual Imagery Questionnaire (KVIQ) for assessing motor imagery in persons with physical disabilities: A reliability and construct validity study. J Neurol Phys Ther 31:20–29.

Mennes M, Kelly C, Zuo X-N, Di Martino A, Biswal BB, Castellanos FX, Milham MP (2010): Inter-individual differences in resting-state functional connectivity predict task-induced BOLD activity. Neuroimage 50:1690–1701.

Mennes M, Kelly C, Colcombe S, Castellanos FX, Milham MP (2013): The extrinsic and intrinsic functional architectures of the human brain are not equivalent. Cereb Cortex 23:223–229.

Mizuguchi N, Nakata H, Hayashi T, Sakamoto M, Muraoka T, Uchida Y, Kanosue K (2013): Brain activity during motor imagery of an action with an object: A functional magnetic resonance imaging study. Neurosci Res 76:150–155.

Mizuguchi N, Yamagishi T, Nakata H, Kanosue K (2015): The effect of somatosensory input on motor imagery depends upon motor imagery capability. Front Psychol 6:1–6.

Oldfield RC (1971): The assessment and analysis of handedness: The Edinburgh inventory. Neuropsychologia 9:97–113.

Piazza M, Izard V (2009): How humans count: Numerosity and the parietal cortex. Neurosci 15:261–273.

Raffin E, Mattout J, Reilly KT, Giraux P (2012): Disentangling motor execution from motor imagery with the phantom limb. Brain 135:582–595.

Di Rienzo F, Collet C, Hoyek N, Guillot A (2014): Impact of neurologic deficits on motor imagery: A systematic review of clinical evaluations. Neuropsychol Rev 24:116–147.

Rushworth MFS, Johansen-Berg H, Göbel SM, Devlin JT (2003): The left parietal and premotor cortices: Motor attention and selection. Neuroimage 20:

Sabaté M, González B, Rodríguez M (2004): Brain lateralization of motor imagery: Motor planning asymmetry as a cause of movement lateralization. Neuropsychologia 42:1041–1049.

Saimpont A, Malouin F, Tousignant B, Jackson PL (2013): Motor imagery and aging. J Mot Behav 45:21–28.

Sharma N, Baron J-C (2013): Does motor imagery share neural networks with executed movement: A multivariate fMRI analysis. Front Hum Neurosci 7:564.

Sharma N, Pomeroy VM, Baron JC (2006): Motor imagery: A backdoor to the motor system after stroke? Stroke 37:1941–1952.

Sharma N, Simmons LH, Jones PS, Day DJ, Carpenter TA, Pomeroy VM, Warburton E. a, Baron JC (2009): Motor imagery after subcortical stroke: A functional magnetic resonance imaging study. Stroke 40:1315–1324.

Simmons L, Sharma N, Baron J-C, Pomeroy VM (2008): Motor imagery to enhance recovery after subcortical stroke: Who might benefit, daily dose, and potential effects. Neurorehabil Neural Repair 22:458–467.

Sirigu A, Duhamel JR, Cohen L, Pillon B, Dubois B, Agid Y (1996): The mental representation of hand movements after parietal cortex damage. Science 273:1564–1568.

Skoura X, Vinter A, Papaxanthis C (2009): Mentally Simulated Motor Actions in Children. Dev Neuropsychol 34:356–367.

Smith SM (2002): Fast robust automated brain extraction. Hum Brain Mapp 17:143–155.

Smith SM, Jenkinson M, Woolrich MW, Beckmann CF, Behrens TEJ, Johansen-Berg H, Bannister PR, De Luca M, Drobnjak I, Flitney DE, Niazy RK, Saunders J, Vickers J, Zhang Y, De Stefano N, Brady JM, Matthews PM (2004): Advances in functional and structural MR image analysis and implementation as FSL. Neuroimage 23:S208–S219.

Smith SM, Fox PT, Miller KL, Glahn DC, Fox PM, Mackay CE, Filippini N, Watkins KE, Toro R, Laird AR, Beckmann CF (2009): Correspondence of the brain's functional architecture during activation and rest. Proc Natl Acad Sci U S A 106: 13040–13045.

Stephan K, Fink G, Passingham R, Silbersweig D, Ceballosbaumann A, Frith C, Frackowiak R (1995): Functional-anatomy of the mental representation of upper extremity movements in healthy-subjects. J Neurophysiol 73: 373–386.

Steyn-Ross ML, Steyn-Ross D. a, Wilson MT, Sleigh JW (2009): Modeling brain activation patterns for the default and cognitive states. Neuroimage 45:298–311.

Stinear CM, Fleming MK, Barber PA, Byblow WD (2007): Lateralization of motor imagery following stroke. Clin Neurophysiol 118:1794–1801.

Szameitat AJ, Shen S, Conforto A, Sterr A (2012a): Cortical activation during executed, imagined, observed, and passive wrist movements in healthy volunteers and stroke patients. Neuroimage 62:266–280.

Szameitat AJ, McNamara A, Shen S, Sterr A (2012b): Neural activation and functional connectivity during motor imagery of bimanual everyday actions. PLoS One 7:

Tacchino A, Bove M, Pedullà L, Battaglia MA, Papaxanthis C, Brichetto G (2013): Imagined actions in multiple sclerosis patients: Evidence of decline in motor cognitive prediction. Exp Brain Res 229:561–570.

Wang YC, Magasi SR, Bohannon RW, Reuben DB, McCreath HE, Bubela DJ, Gershon RC, Rymer WZ (2011): Assessing dexterity function: A comparison of two alternatives for the NIH toolbox. J Hand Ther 24:313–321.

Woolrich MW, Ripley BD, Brady M, Smith SM (2001): Temporal autocorrelation in univariate linear modeling of FMRI data. Neuroimage 14:1370–1386.

Woolrich MW, Jbabdi S, Patenaude B, Chappell M, Makni S, Behrens T, Beckmann C, Jenkinson M, Smith SM (2009): Bayesian analysis of neuroimaging data in FSL. Neuroimage 45: S173–S186.

Zhang H, Long Z, Ge R, Xu L, Jin Z, Yao L, Liu Y (2014): Motor imagery learning modulates functional connectivity of multiple brain systems in resting state. PLoS One 9:e85489.